Functional analysis of CYP2D6.31 variant: Homology modeling suggests possible disruption of redox partner interaction by Arg440His substitution

ARTICLE *in* PROTEINS STRUCTURE FUNCTION AND BIOINFORMATICS · MAY 2005

Impact Factor: 2.63 · DOI: 10.1002/prot.20399 · Source: PubMed

PROTEINS: Structure, Function, and Bioinformatics 59:339–346 (2005)

Functional Analysis of CYP2D6.31 Variant: Homology Modeling Suggests Possible Disruption of Redox Partner Interaction by Arg440His Substitution

Delphine Allorge,[1] Didier Bréant,[1] Jacky Harlow,[2] Joey Chowdry,[2] Jean-Marc Lo-Guidice,[1] Dany Chevalier,[1] Christelle Cauffiez,[1] Michel Lhermitte,[1] Frank E. Blaney,[3] Geoffrey T. Tucker,[2] Franck Broly,[1] and S. Wynne Ellis[2]*

[1]*EA2679, Faculté de Médecine/Pôle Recherche, 59045 Lille, France*
[2]*University of Sheffield, Unit of Molecular and Clinical Pharmacology, Division of Clinical Sciences (South), Royal Hallamshire Hospital, Sheffield, United Kingdom*
[3]*Computational, Analytical and Structural Sciences, GlaxoSmithKline Research and Development, New Frontiers Science Park (North), Third Avenue, Harlow, United Kingdom*

ABSTRACT **Cytochrome P450 2D6 (CYP2D6) is an important human drug-metabolizing enzyme that exhibits a marked genetic polymorphism. Numerous *CYP2D6* alleles have been characterized at a functional level, although the consequences for expression and/or catalytic activity of a substantial number of rare variants remain to be investigated. One such allele, *CYP2D6*31*, is characterized by mutations encoding three amino acid substitutions: Arg296Cys, Arg440His and Ser486Thr. The identification of this allele in an individual with an apparent *in vivo* poor metabolizer phenotype prompted us to analyze the functional consequence of these substitutions on enzyme activity using yeast as a heterologous expression system. We demonstrated that the Arg440His substitution, alone or in combination with Arg296Cys and/or Ser486Thr, altered the respective kinetic parameters [K_m (μM) and k_{cat} (min^{-1})] of debrisoquine 4-hydroxylation (wild-type, 25; 0.92; variants, 43–68; 0.05–0.11) and dextromethorphan *O*-demethylation (wild-type, 1; 4.72; variants, 12–23; 0.64-1.43), such that their specificity constants (k_{cat}/K_m) were decreased by more than 95% compared to those observed with the wild-type enzyme. The rates of oxidation of *rac*-metoprolol at single substrate concentrations of 40 and 400 μM were also markedly decreased by approximately 90% with each CYP2D6 variant containing the Arg440His substitution. These *in vitro* data confirm that the *CYP2D6*31* allele encodes an enzyme with a severely impaired but residual catalytic activity and, furthermore, that the Arg440His exchange alone is the inactivating mutation. A homology model of CYP2D6 based on the crystal structure of rabbit CYP2C5 locates Arg440 on the proximal surface of the protein. Docking the structure of the FMN domain of human cytochrome P450 reductase to the CYP2D6 model suggests that Arg440 is a key member of a cluster of basic amino acid residues important for reductase binding. Proteins 2005;59:339–346.**

Key words: CYP2D6.31; diminished activity; reductase interaction; homology modeling

INTRODUCTION

Cytochrome P450 2D6 (CYP2D6) is an important human drug-metabolizing enzyme involved in the metabolism of many therapeutic agents, including cardiac antiarythmics, β-adrenergic antagonists, antidepressants, antipsychotics and opioid derivatives.[1] This enzyme exhibits a genetic polymorphism, with 5–10% of Caucasians and ≈1% of Asians being deficient in CYP2D6 activity.[2] These so-called poor metabolizer (PM) individuals are homozygous or compound heterozygous for non-functional alleles of *CYP2D6*.[3]

About 15 different inactivating mutations, corresponding to large deletions or point mutations causing splice-site defects or frame shifts, have been described[3] (see also the Human *CYP* Allele Nomenclature website: http://www.imm.ki.se/CYPalleles/cyp2d6.htm). Their identification using polymerase chain reaction (PCR)-based genotyping tests allows the prediction of the PM phenotype of individuals with a high degree of accuracy. Several other allelic variants of the *CYP2D6* gene have also been identified. Many correspond to alleles carrying missense mutations, alone or in combination with other mutations.[4] The consequence of a missense mutation cannot be generally predicted without *in vivo* and/or *in vitro*-generated data. However, depending on the nature and position of the substitution in the protein sequence, some missense mutations can be expected to have an impact on CYP2D6 expression and/or activity. For example, Evert and coworkers[5,6] studied the functional consequence of a His324Pro substitution (*CYP2D6*7* allele), a rare *CYP2D6* missense mutation affecting a strongly conserved P450 residue, and found that this mutation prevents normal protein folding and heme incorporation, leading to an inactive enzyme.

*Correspondence to: Dr. S. Wynne Ellis, Unit of Molecular and Clinical Pharmacology, L-Floor, Division of Clinical Sciences (South), Royal Hallamshire Hospital, Sheffield S10 2JF, UK. E-mail: S.Ellis@Sheffield.ac.uk

Received 14 May 2004; Revised 7 October 2004; Accepted 19 October 2004

Published online 22 February 2005 in Wiley InterScience (www.interscience.wiley.com). DOI: 10.1002/prot.20399

By screening the sequence of the *CYP2D6* gene in a large Caucasian population comprising 672 subjects, we previously identified a rare *CYP2D6* allele (<0.1% allele frequency), named *CYP2D6*31*, which encodes an Arg440His substitution together with Arg296Cys and Ser486Thr exchanges,[4] the latter mutations being found in a number of other alleles, including the functional *CYP2D6*2* allele.[3] We have also recently identified an individual with an apparent PM phenotype with respect to metoprolol oxidation who was originally genotyped by PCR–single strand conformational polymorphism (SSCP) analysis as a compound heterozygote for the *CYP2D6*31* allele and the *CYP2D6*4A* null allele, and, furthermore, was confirmed by sequencing to have no other mutations in the coding regions of the gene. For these reasons, we decided to investigate the consequence of the Arg440His substitution on the activity of the enzyme, both alone and in combination with Arg296Cys and/or Ser486Thr mutations, using three probe substrates of CYP2D6, debrisoquine, dextromethorphan and metoprolol, and recombinant CYP2D6 generated with a yeast heterologous expression system. A homology model of CYP2D6 based on the crystal structure of rabbit CYP2C5 was also constructed and subsequently docked with the crystal structure of the FMN domain of cytochrome P450 reductase in an attempt to rationalize the effect of the mutation(s) at a structural/molecular level.

MATERIALS AND METHODS

Phenotyping of Individual Exhibiting *CYP2D6*4A/*31* Genotype

This individual was a healthy volunteer enrolled in a Phase I clinical trial, totaling 44 Caucasian subjects, thus giving rise to a *CYP2D6*31* allele frequency of approximately 1% in this population sample. Volunteers received a single oral dose of 200 mg *rac*-metoprolol, and the plasma areas under the concentration time-curves of metoprolol and α-hydroxymetoprolol were determined over a 24 h period (AUC_{0-24h}) following administration of the drug, as described by Lennard et al.[7] Individuals with a metoprolol: α-hydroxymetoprolol metabolic ratio (MR) of >12.6 were considered to be poor metabolizers.[8]

Recombinant DNA Manipulation and Generation of Mutant cDNA

Four *CYP2D6* cDNAs encoding (1) an Arg440His mutant, (2) an Arg296Cys/Arg440His double mutant, (3) an Arg440His/Ser486Thr double mutant and (4) an Arg296Cys/Arg440His/Ser486Thr triple mutant were generated with either the Sculptor™ (Amersham International, Little Chalfont, Bucks, U.K.) or the QuikChange™ (Stratagene, Amsterdam, Netherlands) site-directed mutagenesis kits. The point mutations in the wild-type *CYP2D6* cDNA (*CYP2D6*1A*) to generate the above mutant cDNAs were located at, respectively (1) bp 1319 (G→A), (2) bp 886 (C→T) and 1319 (G→A), (3) bp 1319 (G→A) and 1457 (G→C) and (4) bp 886 (C→T), 1319 (G→A) and 1457 (G→C). The base pair numbering is according to the *CYP2D6* cDNA sequence (Genbank accession number NM 000106), the A of ATG start codon being regarded as bp 1. Following successful generation of the mutants, the wild-type and mutated cDNAs were subcloned into the *Bgl* II cloning site of the shuttle expression vector pMA91, as described previously.[9] The presence of the desired mutation(s) and the lack of any additional changes in the *CYP2D6* cDNA were confirmed by sequencing the pMA91 constructs using an automated sequencer (373A, Applied Biosystems, Foster City, CA) and a Taq Dye Deoxy™ Terminator Cycle Sequencing kit (Perkin Elmer, Courtaboeuf, France).

Yeast Microsome Preparation and Spectrophotometric Measurements

Saccharomyces cerevisiae AH22 cells were transformed by electroporation with either the wild-type or mutant CYP2D6 expression constructs. The procedures for transformation, yeast culture and microsome preparation have been described elsewhere.[10] The cytochrome P450 content of yeast-derived microsomes was measured by carbon monoxide-difference spectroscopy[11] and total microsomal protein by the Folin reaction.[12] Binding constants (apparent K_s) were determined from ligand-induced difference spectra using debrisoquine and dextromethorphan according to the method of Jeffcote.[13]

Incubation Conditions and Assays of Debrisoquine, Dextromethorphan and Metoprolol Metabolites

Incubation conditions for the kinetic analyses of debrisoquine and dextromethorphan oxidation over substrate concentrations of 10, 20, 40, 80, 100, 125, 150, 175, 200 μ*M* and 0.5, 1, 2, 5, 10, 20, 40, 60, 80, 100 μ*M*, respectively, and the oxidation of *rac*-metoprolol at low (40 μ*M*) and high (400 μ*M*) substrate concentrations was as described previously.[9,14] Briefly, incubations were initiated by the addition of yeast-derived microsomal preparations containing 20 pmol of CYP2D6 to substrates dissolved in 1.15% (w/v) KCl and an NADPH-generating system comprising 0.4 μmol NADP, 4 μmol glucose 6-phosphate, 2 μmol $MgCl_2$ and 0.4 units of glucose 6-phosphate dehydrogenase dissolved in 0.2 *M* phosphate buffer, pH 7.4. Incubations (0.5 mL final volume) were performed at 37°C for 10 min in a shaking water bath (200 rpm). Linearity of product formation with time and protein concentration was confirmed in preliminary experiments. Control incubations containing the equivalent amount of microsomal protein derived from yeast cells transformed with plasmid lacking *CYP2D6* cDNA were conducted in parallel experiments. High performance liquid chromatography (HPLC) assays for the α-hydroxy and *O*-demethyl metabolites of metoprolol, the 4-hydroxy metabolite of debrisoquine and the *O*-demethyl metabolite of dextromethorphan were carried out according to previously described procedures.[14–16]

Statistical Analysis

Enzyme kinetic parameters (K_m and k_{cat}) for debrisoquine 4-hydroxylation and dextromethorphan *O*-demethylation were determined by Grafit version 3.0 (Erithacus Software Ltd, USA), a data analysis and graphics program

utilizing non-linear regression analysis. The kinetic constant values and rates at single substrate concentrations were compared statistically with ANOVA and the Tukey post hoc test for multiple parameters. A value of $p < 0.05$ was considered statistically significant.

Computational Studies

A homology model of CYP2D6 based on the recently resolved crystal structure of rabbit CYP2C5 (PDB code 1DT6)[17] was constructed. Previous homology models of CYP2D6[18–21] have suffered from a degree of uncertainty because they were based on the crystal structures of bacterial enzymes such as $P450_{BM-3}$ (CYP102) or $P450_{cam}$ (CYP101). CYP2C5 shows a much greater degree of sequence homology to CYP2D6 than bacterial P450s (65% similarity and 42% sequence identity compared to 16% identity with $P450_{BM-3}$) and therefore may be a better template. Sequence alignments of CYP2D6 with CYP2C5 were carried out using the PsiBlast program.[22] The starting model of CYP2D6 was generated manually using the standard homology tools within the Protein Design module of the Quanta program (Quanta 98, Accelrys, La Jolla, CA). Loop regions of the model that were uncertain from the homology were generated and refined using a combined distance geometry-LES (Locally Enhanced Sampling) molecular dynamics refinement that was developed 'in-house.'[23] Use was made of the Karplus rotamer library[24] to refine the side chain dihedrals prior to energy minimization. The latter was achieved with the CHARMm program (version 25.2, Accelrys, La Jolla, CA) with 500 steps of steepest descent and 5000 steps of Adapted Basis Newton Raphson. A dielectric constant of 7.0 was used rather than the more common distance-dependent dielectric to reduce the overwhelming effect of the electrostatic contribution to the energy. Nuclear Overhauser Effect (NOE) distance constraints were used to maintain the fold of the helices and sheet regions. The structure of the FMN binding domain of cytochrome P450 reductase was obtained from the Brookhaven Protein Data Bank (code 1B1C). Charges for the FMN cofactor and the porphyrin heme group were natural atomic orbital charges calculated at the 3-21G* basis set level using the Spartan program (Wavefunction Inc., Irvine, CA). The docking experiments between the CYP2D6 model and reductase were carried out manually within Quanta, and the starting complexes were then minimized with CHARMm using the same protocol as for the homology model itself. Interaction energies between the FMN binding protein and individual residues of CYP2D6 were calculated with CHARMm as the sum of electrostatic and Van der Waals terms. In these calculations, the more common distance-dependent dielectric was used for the electrostatics.

RESULTS AND DISCUSSION

Phenotype of Individual with *CYP2D6*4A/*31* Genotype

AUC_{0-24h} of metoprolol and α-hydroxymetoprolol in the individual genotyped as *CYP2D6*4A/**31 were 4899 and 367 ng.h mL^{-1}, respectively, resulting in a metoprolol MR of 13.3. The corresponding mean AUC_{0-24h} of volunteers ($n = 29$) genotyped as homozygous or hererozygous wild-type (extensive metabolizer, EM) were 1437 ± 861 and 1394 ± 331 ng.h mL^{-1}, respectively, giving a mean MR of 1.3 ± 1.0. Four other volunteers, genotyped as unambiguous PMs due to the presence of known null alleles occurring either in a homozygous or compound heterozygous state, had a mean metoprolol AUC_{0-24h} of 5341 ± 1958 ng.h mL^{-1}, although the plasma level of α-hydroxymetoprolol was below the limit of quantification.

TABLE I. Type 1 Binding Coefficients (K_s) of Debrisoquine and Dextromethorphan with Wild-type and Variant Forms of CYP2D6

	K_s (μ*M*)		
Ligand	CYP2D6.1	CYP2D6.31	CYP2D6–Arg440His
Debrisoquine	25.8 ± 3.9	36.8 ± 8.4	34.5 ± 3.0
Dextromethorphan	6.9 ± 0.3	5.8 ± 0.7	5.0 ± 0.7

Values are means ±SD for three determinations.

Spectral Characterization of Recombinant CYP2D6 Enzymes

The P450 holoprotein content, as determined by CO-difference spectroscopy, of microsomes prepared from yeast cells expressing the wild-type and mutant forms of CYP2D6 was relatively similar (mean, 45; range, 28–57 pmol of P450 per milligram of microsomal protein). Each P450 spectrum exhibited a Soret absorption maximum at 448 nm, and no P420 peak was detectable (data not shown). Debrisoquine- and dextromethorphan-induced difference spectra (type I) demonstrated that the Arg440His mutation, either alone or in combination with Arg296Cys and Ser486Thr, did not significantly alter the binding capacity of the enzyme for the substrates, as shown in Table I.

CYP2D6 Enzymatic Activities Using Debrisoquine, Dextromethorphan and Metoprolol

Compared to that of the wild-type enzyme, the apparent K_m values of the mutant enzymes containing the Arg440His substitution, either alone or in combination with Arg296Cys and/or Ser486Thr, were two- to three-fold higher for debrisoquine 4-hydroxylation, and 9- to 17-fold higher for dextromethorphan *O*-demethylation (Tables II and III). Each form of mutant containing the Arg440His mutation also exhibited a significant decrease in k_{cat} values for the oxidation of both substrates (5–30% of wild-type), giving rise to severely decreased specificity constant (k_{cat}/K_m) values, which were about 4% of the CYP2D6.1 value with debrisoquine and 2% with dextromethorphan (Tables II and III). The rates of *rac*-metoprolol oxidation by each form of mutant at both low (40 μ*M*) and high (400 μ*M*) substrate concentrations were also markedly reduced by approximately 90% of the wild-type activity (Table IV).

TABLE II. Calculated Michaelis-Menten Parameters for Debrisoquine 4-hydroxylation by Wild- type and Variant Forms of CYP2D6

Enzyme	k_{cat} (min^{-1})	K_m (μM)	k_{cat}/K_m (min^{-1} mM^{-1})
Wild-type (CYP2D6.1)	0.92 ± 0.12	25 ± 2	37.57 ± 3.21
Arg440His	0.08 ± 0.01	49 ± 9	1.55 ± 0.06
Arg440His + Arg296Cys	0.11 ± 0.01	68 ± 17	1.72 ± 0.31
Arg440His + Ser486Thr	0.05 ± 0.01	43 ± 23	1.28 ± 0.43
Arg440His + Arg296Cys + Ser48Thr (CYP2D6.31)	0.09 ± 0.01	60 ± 14	1.48 ± 0.17

Values are means ±SD for three experiments, each experiment comprising two replicates.

TABLE III. Calculated Michaelis–Menten Parameters for Dextromethorphan *O*-demethylation by Wild-type and Variant Forms of CYP2D6

Enzyme	k_{cat} (min^{-1})	K_m (μM)	k_{cat}/K_m (min^{-1} μM^{-1})
Wild-type (CYP2D6.1)	4.72 ± 0.58	1.4 ± 0.5	3.65 ± 1.02
Arg440His	0.83 ± 0.03	11.7 ± 8.3	0.10 ± 0.06
Arg440His + Arg296Cys	1.18 ± 0.03	22.8 ± 5.7	0.05 ± 0.01
Arg440His + Ser486Thr	0.64 ± 0.09	11.6 ± 7.3	0.08 ± 0.05
Arg440His + Arg296Cys + Ser486Thr (CYP2D6.31)	1.43 ± 0.11	17.9 ± 9.2	0.08 ± 0.04

Values are means ±SD for three experiments, each experiment comprising two replicates.

TABLE IV. Oxidation of *rac*-Metoprolol by Wild-type and Variant Forms of CYP2D6

	α-Hydroxylation		*O*-Demethylation	
	(pmol/min/pmol P450)			
Enzyme	40 μM	400 μM	40 μM	400 μM
Wild-type (CYP2D6.1)	0.63	1.02	2.09	3.34
Arg440His	0.06 (10%)	0.12 (12%)	0.20 (10%)	0.41 (12%)
Arg440His + Arg296Cys	0.05 (8%)	0.14 (14%)	0.17 (8%)	0.45 (13%)
Arg440His + Ser486Thr	0.05 (8%)	0.11 (11%)	0.13 (6%)	0.31 (9%)
Arg440His + Arg296Cys + Ser486Thr (CYP2D6.31)	0.05 (8%)	0.13 (13%)	0.20 (10%)	0.41 (12%)

Values are means for two experiments, each experiment comprising three replicates. Values in parentheses are percents of wild-type.

Homology Model of CYP2D6 and Docking with Reductase

The rabbit CYP2C5 crystal structure was used as a template for homology modeling of CYP2D6. Due to the high degree of amino acid sequence similarity between CYP2D6 and CYP2C5, only minor insertions or deletions were necessary in the construction of the CYP2D6 model. Some recent work has suggested that the B-C loop in particular is more similar in homology to the $P450_{BM-3}$ structure and that Asp301 is playing a structural role in hydrogen bonding to the backbone NH hydrogens of Val119 and Phe120.[25] Our model does not support this hypothesis, and furthermore, in the same study by Paine et al.[25] it was shown that CYP2D6 with an Asp301Glu mutation still retained substantial catalytic activity. This would suggest that the proposed structural role for Asp301 is open to question, as the equivalent Glu301 cannot form the same hydrogen bonds to Val119 and Phe120.

In our homology model of CYP2D6, Arg296 is located on the I-helix close to the distal surface of the protein (Fig. 1) and remote from the active site. Likewise, Ser486 is on a surface β-strand (β4-2), close to the C-terminal domain and is again distant from the active site. Arg440 is also remote from the active site, but is located on a turn along with Arg441, a highly conserved residue in the vast majority of P450s that forms a salt bridge with the carboxyl group of pyrrole ring A of the heme (Fig. 1). The side chain of Arg440 projects outward from the proximal surface of the protein into the region that could form the binding interface with cytochrome P450 reductase. This interface area contains a cluster of other basic residues, including Arg62, Arg63, Arg88, Arg129, Arg132, Arg133, Arg140 and Arg450, in addition to Arg440 (several of these are shown in Fig. 1). The crystal structure of the FMN binding domain of human cytochrome P450 reductase shows a large number of acidic residues close to the FMN cofactor that could interact with the aforementioned basic residues of CYP2D6.[26] In fact, the electrostatic potential surfaces of the two proteins, as calculated using the Grasp Poisson–Boltzmann method, show a high degree of comple-

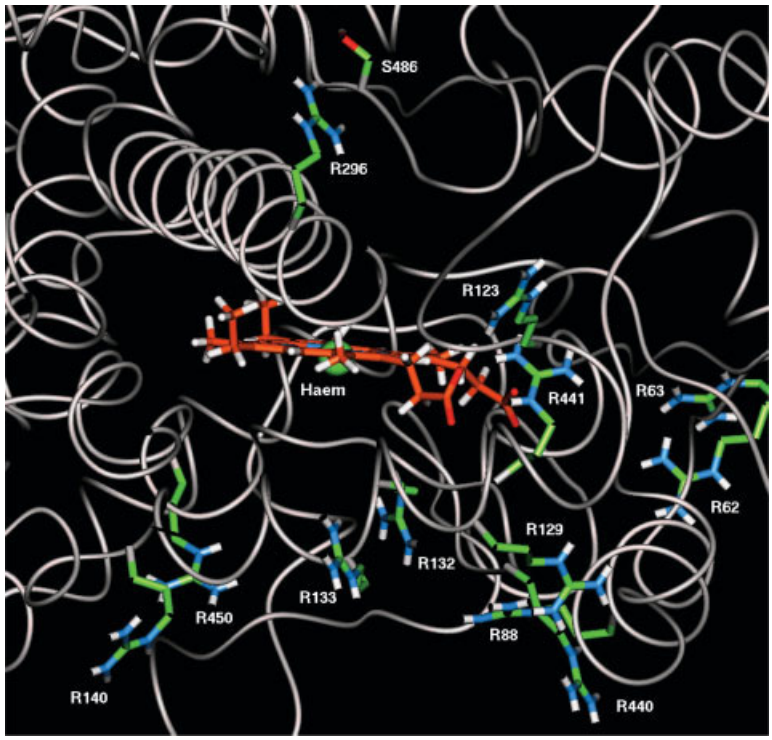

Fig. 1. Homology model of CYP2D6 showing the positions of Arg(R)296, Arg(R)440 and Ser(S)486 that are mutated in CYP2D6.31 and the cluster of arginine residues on the proximal surface of the protein. Arg(R)441 is a highly conserved residue that interacts with one of the propionate side chains of the heme (shown in red).

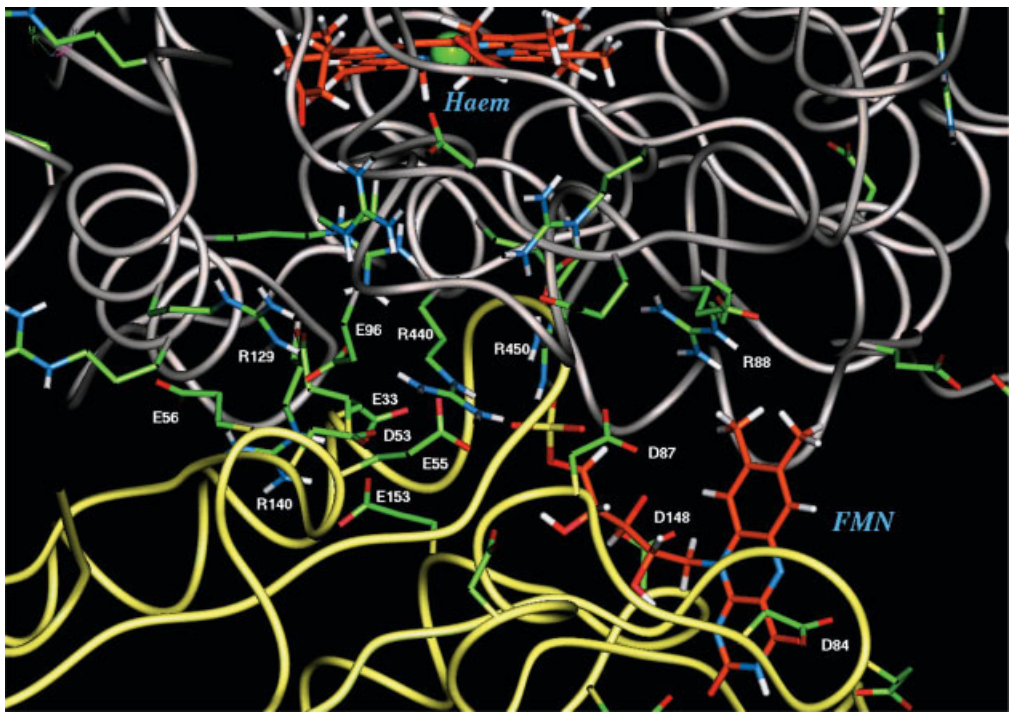

Fig. 2. The interface region of CYP2D6 (gray coil) and cytochrome P450 reductase (yellow coil) showing many of the salt bridges that form in this region. Arg(R)440 interacts closely with Asp(D)53 and Glu(E)55 of the reductase and Glu(E)96 of the P450 (see text for details).

TABLE V. Energy Contributions (Electrostatic, Van der Waals and Total [Kcal/mol]) to the Interactions Between CYP2D6 and the FMN Binding Protein, as Calculated by CHARMm

No.	Interaction Between	Electrostatic	VdW	Total
1	CYP2D6 and FMN BP with Arg440 ⇔ Asp148	−22.53	−113.10	−135.63
2	CYP2D6 and FMN BP with Arg440 ⇔ Asp84/Asp87	−23.86	−82.64	−106.49
3	CYP2D6 and FMN BP with Arg440 ⇔ Asp53/Glu55	−224.97	−149.71	−374.68
4	Arg62 and FMN BP	0.00049	0.0	0.0
5	Arg63 and FMN BP	0.0	0.0	0.0
6	Arg64 and FMN BP	0.0	0.0	0.0
7	Arg88 and FMN BP	−1.97	−5.22	−7.19
8	Arg129 and FMN BP	−19.39	−6.16	−25.55
9	Arg132 and FMN BP	−36.47	−5.77	−42.24
10	Arg133 and FMN BP	25.82	−9.29	16.52
11	Arg140 and FMN BP	−25.30	−7.89	−33.20
12	Arg440 and FMN BP	−59.68	−12.14	−71.82
13	Arg450 and FMN BP	−12.78	−2.14	−14.92
14	Arg440His and FMN BP	−6.34	−7.28	−13.63

The first three rows are the interaction energies between the two proteins with Arg440 of CYP2D6 docked to each of the three acidic clusters of FMN binding protein (FMN BP) as discussed in the results. Rows 4–13 shows the interactions between each of the arginines in the interface region and FMN BP, when the two proteins are docked in the most favored conformation. The final row 14 shows the greatly reduced interaction energy of the Arg440His mutant compared to the wild-type (row 12).

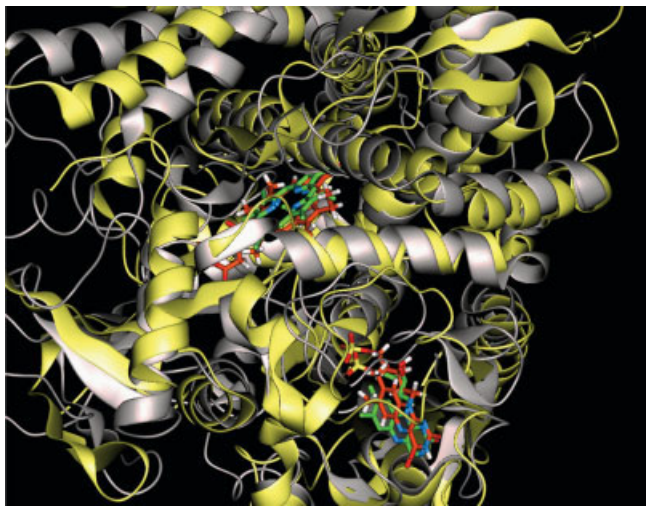

Fig. 3. An root mean square (RMS)-fitted overlay of the CYP2D6–reductase model complex (proteins, gray; porphyrin and FMN cofactors, orange) with the crystal structure of the bacterial cytochrome $P450_{BM-3}$ bound to its reductase (proteins, yellow; porphyrin and FMN cofactors, green). Note the excellent overlap of the porphyrin rings and the FMN cofactors, together with the close proximity of the equivalent helices. The I-helices can be seen just above the porphyrin rings of the complexes.

mentarity with the highly basic cytochrome P450 regions matching acidic regions of the reductase (data not shown). Because of this, a series of docking experiments between CYP2D6 and the reductase FMN binding domain were conducted in order to ascertain the best possible interaction between Arg440 and one or more of the acidic residues of the reductase. Docking Arg440 with Asp148 of the reductase, a residue previously shown to reduce CYP2D6-mediated codeine *O*-demethylation by 70% when mutated to Asn,[26] was found to lead to a large number of steric clashes, and the overall protein–protein interaction was largely unfavorable. Full minimization of this complex resulted in the relatively low electrostatic contribution of −22.53 Kcal/mol to the overall binding energy (Table V). Another region of the reductase that has been shown, upon mutation, to reduce codeine *O*-demethylation was the β3-α5 loop containing residues Asp84 and Asp87.[26] Docking of the Arg440 region towards these residues again gave a number of unfavorable interactions, although less so than in the initial docking experiment. Minimization of this complex, however, led to a less favorable Van der Waals contribution, and therefore this was also rejected (Table V). Our final docking study led to Arg440 interacting with the β2-α3 residues, Asp53 and Glu55 of the reductase (Fig. 2). This protein–protein interface was found to be highly favorable, having a 10-fold higher electrostatic contribution compared to the interactions with Asp148 or Asp84/Asp87, resulting in an overall binding energy of −374.68 Kcal/mol (Table V). Furthermore, in this docking orientation, Arg440 not only appears to be tightly bound to Asp53 and Glu55 but also to Glu96 of CYP2D6. Other salt bridges are also observed [e.g. Arg140 forms an interaction with Glu153 of the reductase (Fig. 2)]. Supportive evidence for this docking conformation could also be found when the model complex was compared with the crystal structure of the bacterial $P450_{BM-3}$/FMN binding domain protein (Brookhaven code 1BVY) reported by Sevrioukova.[27] Despite low sequence identity, the CYP2D6 homology model and the $P450_{BM-3}$ crystal structure have very similar folds. When the two P450 proteins were superimposed, there was an excellent overlap between the positions of the hemes and the FMN cofactors (Fig. 3).

Discussion

The initial goal of the present study was to investigate the functional consequence of the three amino acid substitutions, Arg296Cys, Arg440His and Ser486Thr associated with the rare *CYP2D6*31* allele. This was undertaken because of the identification of an individual exhibiting an apparent PM phenotype with respect to metoprolol oxidation who was genotyped as a compound heterozygote for the *CYP2D6*31* allele and the most frequent non-functional *CYP2D6*4A* allele. Although the phenotyping of this individual showed detectable plasma levels of α-hydroxymetoprolol, as opposed to levels below the limit of detection in unambiguous PMs, the AUC_{0-24h} of plasma metoprolol was comparable to that found in the known PMs, and approximately four-fold greater than that associated with EM volunteers. Furthermore, the metoprolol MR (13.3) of the individual was greater than the antimode MR of 12.6 associated with PM individuals.[8] Overall, therefore, the phenotyping data of the volunteer genotyped as *CYP2D6*4A/*31* are consistent with a PM status.

However, the *in vitro* catalytic activity data indicate that although the enzyme encoded by the *CYP2D6*31*

allele is severely impaired, it still retains some residual activity, its catalytic efficiency (k_{cat}/K_m) towards debrisoquine and dextromethorphan approaching 2–4% of that of the wild-type enzyme. This residual activity prompts the question of whether *CYP2D6*31* can truly be regarded as a PM allele. Other alleles, such as *CYP2D6*9* and *CYP2D6*10,* also result in the expression of variant enzymes with similarly impaired levels of *in vitro* catalytic activity.[28–30] Furthermore, in contrast to CYP2D6.31, the levels of expression of functional holoenzyme are markedly reduced due to poor heme incorporation/instability.[31–33] In an *in vivo* context, *CYP2D6*9* and *CYP2D6*10* are regarded as intermediate metabolizer (IM) alleles,[33] and therefore by comparison *CYP2D6*31* cannot be unequivocally characterized as a PM allele from the *in vitro* data presented in this study, despite the implication of the *in vivo* phenotyping data.

Nevertheless, the *in vitro* data clearly show that Arg440His alone is the debilitating mutation responsible for the diminished activity of CYP2D6.31. The comparable holoenzyme content of wild-type and mutant enzymes indicate that the reduced activity of CYP2D6.31 is unlikely to be due to the Arg440His substitution affecting heme incorporation through a gross structural effect. Neither is it due to a reduction in the substrate-binding capacity of the mutant enzyme, this being demonstrated by the similar debrisoquine and dextromethorphan binding coefficients with the wild-type enzyme. Although not tested specifically in this investigation, through inference the Arg296Cys and/or Ser486Thr mutations associated with the *CYP2D6*31* allele do not appear to have any marked effect on the level of expression and catalytic activity of the CYP2D6.31 enzyme. This inference is supported by our homology model: being remote from the active site, these two residues would not be anticipated to have a marked functional/structural consequence when substituted. However, although a number of publications report *in vitro* or *in vivo* data that support our proposition that these two substitutions do not markedly affect the catalytic activity of the enzyme,[33–38] there are contradictions in the literature[30,39] reporting three- to five-fold decreases in the catalytic efficiency of the enzyme relative to wild-type.

In contrast to Arg296 and Ser486, Arg440 is critical for catalytic activity, and according to our homology model of CYP2D6 is ideally positioned on the proximal surface of the enzyme to interact with its redox partner, cytochrome P450 reductase. Computational docking experiments between the homology model of CYP2D6 and the crystal structure of the FMN binding domain of human cytochrome P450 reductase were undertaken to further investigate this proposal. The docking experiments discounted interactions between Arg440 and Asp148 or Asp84/Asp87 in the binding interface between the two proteins on the grounds of initial steric clashes and low overall electrostatic interaction energies following minimization. In contrast, the interaction between Arg440 and Asp53/Glu55 of the reductase appeared to be highly favorable (Fig. 2; Table V), showing minimal steric clashes and an overall electrostatic interaction 10-fold greater than the interactions with Asp148 or Asp84/Asp87. Unfortunately, no mutation studies have been reported for Asp53/Glu55 of the reductase to confirm their importance in such an interaction.

From the experimental data, it is not possible to determine whether Arg440 is involved directly in the transfer of electrons from the reductase to the P450. However, the computational modeling would suggest that this might not be the case since salt bridges between Arg440 and Asp53/Glu55 are fairly remote from the FMN cofactor (Fig. 2). It is suggested therefore that Arg440 is more likely to act as a primary binding site in the interface between the P450 and reductase, ensuring appropriate orientation/geometry for efficient electron transfer via other residue interactions. In this regard, Figure 2 reveals that Asp148 of the reductase, which has been shown to have the greatest effect on CYP2D6-mediated codeine *O*-demethylation,[26] is bound directly to the FMN cofactor.[26] This cofactor comes within reasonable distance of Arg450 of CYP2D6 (Fig. 2) and could form a hydrogen bond network to it, through some water molecules. It is thus more likely that this Arg450 is involved in electron transfer.

The proposed role of Arg440 in reductase binding is further supported by the energy calculations of the contribution of individual arginine residues to reductase binding, Arg440 forming the strongest (−71.82 Kcal/mole) overall interaction with the reductase (Table V). The Arg440His exchange, responsible for the diminished catalytic activity of CYP2D6.31, reduces the interaction energy by over 58 Kcal/mole (Table V), a reflection of histidine's weaker base properties, in addition to the inability of its shorter side chain to come into close proximity with the acidic residues of the reductase. Thus the binding between CYP2D6 and its reductase is likely to be severely reduced/altered with a subsequent detrimental effect on electron transfer and hence catalytic activity.

To our knowledge, no other report has appeared in the literature describing the influence of the Arg440His substitution on CYP2D6 catalytic activity. However, Lys453 of rat CYP1A2 aligns with Arg440 of CYP2D6,[40] and there are numerous reports describing the inhibitory effect of a Lys453Glu exchange on CYP1A2 catalytic activity.[41–43] This substitution apparently lowers the affinity of the reductase for CYP1A2, suggesting that it may play a role in anchoring the reductase to the P450 to ensure proper geometry of the proteins for electron transfer.[43] Hence, the proposed role of Arg440 of CYP2D6 in reductase binding is compatible with published data of an analogous residue found in a different mammalian P450.

REFERENCES

1. Wolf CR, Smith G. Pharmacogenetics. Br Med Bull 1999;55:366–386.
2. Gaedigk A. Interethnic differences of drug-metabolizing enzymes. Int J Clin Pharmacol Ther 2000;38:61–68.
3. Daly AK, Brockmöller J, Broly F, Eichelbaum M, Evans WE, Gonzalez FJ, Huang JD, Idle JR, Ingelman-Sundberg M, Ishizaki T, Jacqz-Aigrain E, Meyer UA, Nebert DW, Steen VM, Wolf CR, Zanger UM. Nomenclature for human CYP2D6 alleles. Pharmacogenetics 1996;6:193–201.
4. Marez D, Legrand M, Sabbagh N, Lo-Guidice J-M, Spire C, Lafitte J-J, Meyer UA, Broly F. Polymorphism of the cytochrome P450 CYP2D6 gene in a European population: characterization of 48 mutations and 53 alleles, their frequencies and evolution. Pharmacogenetics 1997;7:193–202.
5. Evert B, Griese EU, Eichelbaum M. A missense mutation in exon 6

of the CYP2D6 gene leading to a histidine 324 to proline exchange is associated with the poor metabolizer phenotype of sparteine. Naunyn-Schmiedeberg's Arch Pharmacol 1994;350:434–439.
6. Evert B, Eichelbaum M, Haubruck H, Zanger UM. Functional properties of CYP2D6 1 (wild-type) and CYP2D6 7 ($His_{324}Pro$) expressed by recombinant baculovirus in insect cells. Naunyn-Schmiedeberg's Arch Pharmacol 1997;355:309–318.
7. Lennard MS, Silas JH, Freestone S, Ramsay LE, Tucker GT, Woods HF. Oxidation phenotype – a major determinant of metoprolol metabolism and response. N Engl J Med 1982;307:1558–1560.
8. McGourty JC, Silas JH, Lennard MS, Tucker GT, Woods HF. Metoprolol metabolism and debrisoquine oxidation polymorphism: population and family studies. Br J Clin Pharmacol 1985;20:555–566.
9. Ellis SW, Rowland K, Ackland MJ, Rekka E, Simula AP, Lennard MS, Wolf CR, Tucker GT. Influence of amino acid residue 374 of cytochrome *P*-450 2D6 (CYP2D6) on the regio- and enantioselective metabolism of metoprolol. Biochem J 1996;316:647–654.
10. Ellis SW, Hayhurst GP, Lightfoot T, Smith G, Harlow J, Rowland-Yeo K, Larsson C, Mahling J, Lim CK, Wolf CR, Blackburn MG, Lennard MS, Tucker GT. Evidence that serine 304 is not a key ligand-binding residue in the active site of cytochrome P450 2D6. Biochem J 2000;345:565–571.
11. Omura T, Sato R. The carbon monoxide-binding pigment of liver microsomes I. Evidence for its hemoprotein nature. J Biol Chem 1964;239:2370–2378.
12. Lowry OH, Rosebrough NJ, Farr AL, Randall RJ. Protein measurement with the Folin phenol reagent. J Biol Chem 1951;193:265–275.
13. Jeffcote CR. Measurement of substrate and inhibitor binding to microsomal cytochrome P-450 by optical-difference spectroscopy. Methods Enzymol 1978;52:258–279.
14. Lightfoot T, Ellis SW, Mahling J, Ackland MJ, Blaney FE, Biljoo GJ, de Groot MJ, Vermeulen NPE, Blackburn GN, Lennard MS, Tucker GT. Regioselective hydroxylation of debrisoquine by cytochrome P450 2D6: implications for active site modelling. Xenobiotica 2000;30:219–233.
15. Otton SV, Crewe HK, Lennard MS, Tucker GT, Woods HF. Use of quinidine inhibition to define the role of the sparteine/debrisoquine cytochrome P450 in metoprolol oxidation by human liver microsomes. J Pharmacol Exp Ther 1988;247:242–247.
16. Chen ZR, Somogyi AA, Bochner F. Simultaneous determination of dextromethorphan and three metabolites in plasma and urine using high-performance liquid chromatography with application to their disposition in man. Ther Drug Monit 1990;12:97–104.
17. Williams PA, Cosme J, Stridhar V, Johnson EF, McRee DE. Mammalian microsomal cytochrome P450 monoxygenase: structural adaptations for membrane binding and functional diversity. Mol Cell 2000;5:121–131.
18. Modi S, Paine MJ, Sutcliffe MJ, Lian L-Y, Primrose WU, Wolf CR, Roberts GCK. A model for human cytochrome P450 2D6 based on modelling and NMR studies of substrate binding. Biochemistry 1996;35:4540–4550.
19. Lewis DFV, Eddershaw PJ, Goldfarb PS, Tarbit MH. Molecular modelling of cytochrome P450 2D6 (CYP2D6) based on alignment with CYP102: structural studies on specific CYP2D6 substrate metabolism. Xenobiotica 1997;27:319–340.
20. de Groot MJ, Ackland MJ, Horne VA, Alex AA, Jones BC. Novel approach to predicting P450-mediated drug metabolism: development of a combined protein and pharmacophore model for CYP2D6. J Med Chem 1999;42:1515–1524.
21. de Rienzo F, Fanelli F, Menziani C, de Benedetti PG. Theoretical investigation of substrate specificity for cytochromes P450 IA2, P450 IID6 and P450 IIIA4. J Comp Aided Mol Design 2000;14:93–116.
22. Altschul SF, Madden TL, Schaffer AA, Zhang J, Zhang Z, Miller W, Lipman DJ. Gapped BLAST and PSI-BLAST: a new generation of protein database search programs. Nucleic Acids Res 1997;25:3389–3402.
23. Blaney FE, Raveglia LF, Artico M, Cavagnera S, Dartois C, Farina C, Grugni M, Gagliardi S, Luttmann MA, Martinelli M, Nadler GM, Parini C, Petrillo P, Sarau HM, Scheideler MA, Hay DWP, Giardina GAM. Stepwise modulation of neurokinin-3 and neurokinin-2 receptor affinity and selectivity in quinoline tachykinin receptor antagonists. J Med Chem 2001;44:1675–1689.
24. Dunbrack RL Jr, Karplus M. Backbone-dependent rotamer library for proteins. Application to side-chain prediction. J Mol Biol 1993;230:543–574.
25. Paine MJ, McLaughlin LA, Flanagan JU, Kemp CA, Sutcliffe MJ, Roberts GCK, Wolf CR. Residues glutamate 216 and aspartate 301 are key determinants of substrate specificity and product regioselectivity in cytochrome P450 2D6. J Biol Chem 2003;278:4021–4027.
26. Zhao Q, Modi S, Smith G, Paine M, McDonagh PD, Wolf CR, Tew D, Lian L-Y, Roberts GCK, Driessen HPC. Crystal structure of the FMN-binding domain of human cytochrome P450 reductase at 1.93 Ang resolution. Prot Sci 1999;8:298–306.
27. Sevrioukova IF, Li H, Zhang H, Peterson JA, Poulos TL. Structure of a cytochrome P450-redox partner electron-transfer complex. Proc Natl Acad Sci USA 1999;96:1863–1868.
28. Broly F, Meyer UA. Debrisoquine oxidation polymorphism: phenotypic consequences of a 3-base-pair deletion in exon 5 of the *CYP2D6* gene. Pharmacogenetics 1993;3:123–130.
29. Ramamoorthy Y, Tyndale RF, Sellers EM. Cytochrome P450 2D6.1 and cytochrome P450 2D6.10 differ in catalytic activity for multiple substrates. Pharmacogenetics 2001;11:477–487.
30. Yu A, Kneller BM, Rettie AE, Haining RL. Expression, purification, biochemical characterization, and comparative function of human cytochrome P450 2D6.1, 2D6.2, 2D6.10, and 2D6.17 allelic isoforms. J Pharmacol Exp Ther 2002;303:1291–1300.
31. Johansson I, Oscarson M, Yue QY, Sjoqvist F, Ingelman-Sundberg M. Genetic analysis of the Chinese cytochrome P4502D locus: characterization of variant *CYP2D6* genes present in subjects with diminished capacity for debrisoquine hydroxylation. Mol Pharmacol 1994;46:452–459.
32. Fukuda T, Nishida Y, Imaoka S, Hiroi T, Naohara M, Funae Y, Azuma J. The decreased *in vivo* clearance of CYP2D6 substrates by CYP2D6*10 might be caused not only by the low-expression but also by low affinity of CYP2D6. Arch Biochem Biophys 2000;380:303–308.
33. Zanger UM, Fischer J, Raimundo S, Stüven T, Evert BO, Schwab M, Eichelbaum M. Comprehensive analysis of the genetic factors determining expression and function of hepatic CYP2D6. Pharmacogenetics 2001;11:573–585.
34. Morita S, Shimoda K, Someya T, Yoshimura Y, Kamijima K, Kato N. Steady-state plasma levels of nortriptyline and its hydroxylated metabolites in Japanese patients: impact of CYP2D6 genotype on the hydroxylation of nortriptyline. J Clin Psychopharmacol 2000;20:141–149.
35. Wennerholm A, Johansson I, Hidestrand M, Bertilsson L, Gustafsson LL, Ingelman-Sundberg M. Characterization of the CYP2D6*29 allele commonly present in a black Tanzanian population causing reduced catalytic activity. Pharmacogenetics 2001;11:417–427.
36. Tsuzuki D, Takemi C, Yamamoto S, Tamagake K, Imaoka S, Funae Y, Kataoka H, Shinoda S, Narimatsu S. Functional evaluation of cytochrome P450 2D6 with Gly42Arg substitution expressed in *Saccharomyces cerevisiae*. Pharmacogenetics 2001;11:709–718.
37. Bapiro TE, Hasler JA, Ridderström M, Masimirembwa CM. The molecular and kinetic basis for the diminished activity of cytochrome P450 2D6.17 (CYP2D6.17) variant – potential implications for CYP2D6 phenotyping studies and the clinical use of CYP2D6 substrate drugs in some African populations. Biochem Pharmacol 2002;64:1387–1398.
38. Marcucci KA, Pearce RE, Crespi C, Steimel DT, Leeder JS, Gaedigk A. Characterisation of cytochrome P450 2D6.1 (CYP2D6), CYP2D6.2, and CYP2D6.17 activities toward model substrates dextromethorphan, bufuralol, and debrisoquine. Drug Metab Dispos 2002;30:595–601.
39. Shimada T, Tsumura F, Yamazaki H, Guengerich FP, Inoue K. Characterization of (±)-bufuralol hydroxylation activities in liver microsomes of Japanese and Caucasian subjects genotyped for CYP2D6. Pharmacogenetics 2001;11:143–156.
40. Lewis DFV. Three-dimensional models of human and other mammalian microsomal P450s constructed from an alignment with P450102 ($P450_{bm3}$). Xenobiotica 1995;25:333–366.
41. Furuya H, Shimizu T, Hirano K, Fujii-Kuriyama Y, Raag R, Poulos TL. Site-directed mutagenesis of rat cytochrome $P\text{-}450_d$: catalytic activities toward benzphetamine and 7-ethoxycoumarin. Biochemistry 1989;28:6848–6857.
42. Shimizu T, Sadeque AJM, Sadeque GN, Hatano M, Fujii-Kuriyama Y. Ligand binding studies of engineered cytochrome $P\text{-}450_d$ wild type, proximal mutants, and distal mutants. Biochemistry 1991;30:1490–1496.
43. Shimizu T, Tateishi T, Hatano M, Fujii-Kuriyama Y. Probing the role of lysines and arginines in the catalytic function of cytochrome $P450_d$ by site-directed mutagenesis. J Biol Chem 1991;266:3372–3375.